ISSN 1063-7834, Physics of the Solid State, 2016, Vol. 58, No. 6, pp. 1154–1159. © Pleiades Publishing, Ltd., 2016.
Original Russian Text © A.S. Elshin, D.A. Abdullaev, E.D. Mishina, 2016, published in Fizika Tverdogo Tela, 2016, Vol. 58, No. 6, pp. 1118–1123.

FERROELECTRICITY

Dependence of the Optimum Parameters of Femtosecond Laser Annealing of Lead Zirconate Titanate Films on Their Thickness

A. S. Elshin*, D. A. Abdullaev, and E. D. Mishina

Moscow State Technical University of Radio Engineering, Electronics, and Automation, pr. Vernadskogo 78, Moscow, 119454 Russia

** e-mail: elshin_andrew@mail.ru*

Received October 27, 2015

Abstract—The optimum parameters of laser annealing (crystallization) induced by repetitive pulses with a pulse duration of 100 fs and a wavelength of 800 nm, which falls in the transparency region of the film and, simultaneously, in the absorption region of the substrate, have been investigated experimentally as a function of the thickness of the ferroelectric film. It has been shown that, with an increase in the thickness of the ferroelectric film by 100 nm (in the range from 300 to 600 nm), the required power density of the laser beam increases, on the average, by 0.1 MW/cm^2. The optimum exposure time of the laser beam with the desired power increases nonlinearly with an increase in the thickness of the film.

DOI: 10.1134/S1063783416060147

1. INTRODUCTION

The integration of thin-film ferroelectrics into the silicon technology holds much promise, but it is not a simple problem due to the occurrence of interfacial chemical reactions and the interlayer diffusion of atoms under the necessary conditions for crystallization [1, 2]. The crystallization of a ferroelectric phase requires the use of high temperatures (usually, 500°C and higher). There is frequently a need to avoid heating of the structure as a whole. In this case, the ferroelectric is subjected to local influences. A local annealing can be achieved by different methods (for example, using a hot cantilever or laser heating). The use of the hot cantilever method leads to a local heating of the film, which makes it possible to perform crystallization of local regions. For successful crystallization, it is common practice to use either the preliminary heating of the sample to temperatures in the range from 250 to 300°C [3] or an electric field applied between the cantilever and the sample [4]. The disadvantage of this method of annealing is the lack of "flexibility" of the process, because the heat source is always located on the surface. A laser annealing provides a means for crystallization of local regions without preliminary heating (when the maximum evaporation temperature of the precursor is as high as 150°C). Moreover, it is possible to use different heating regimes with a heat source on the surface or in the bulk of the film, depending on the parameters of the radiation. A local laser heating does not affect the surrounding regions, because they are free of temperature-induced defects. Research works on the laser annealing of ferroelectric materials were started in the 1980s [5]. In the majority of the works carried out in this period, a continuous-wave CO_2 laser was used as the heat source providing annealing in a 0.5×0.5 mm region of the ferroelectric film. In the case where an excimer laser was used as the heat source, the crystallization region was located on the surface, whereas the lower part of the ferroelectric film remained amorphous. The remanent polarization of the ferroelectric material upon annealing with a CO_2-laser radiation proved to be seven times higher than that in the case of a KrF-excimer-laser annealing. Furthermore, the use of a continuous-wave CO_2 laser resulted in a more homogeneous crystallization [6]. Subsequently, local annealings of semiconductor materials were also implemented using pulsed femtosecond lasers [7], which ensured a high heating rate and a rapid crystallization with minor defects. A rapid annealing is of interest in connection with the decrease in the degree of undesirable interlayer diffusion and the number of other defects, as well as the diffusion of impurities, especially in the case of semiconductors. For lead-containing materials, such as lead zirconate titanate (PZT), a rapid heating leads to a smaller loss of volatile lead [8]. Interest in this subject today is also maintained at a high level (see, for example, [9–11]) owing to the investigations of local features in the kinetics of phase transitions in nanoscale ferroelectrics, as well as the prospects for practical application of techniques in the field of micro- and nanoelectronic technologies.

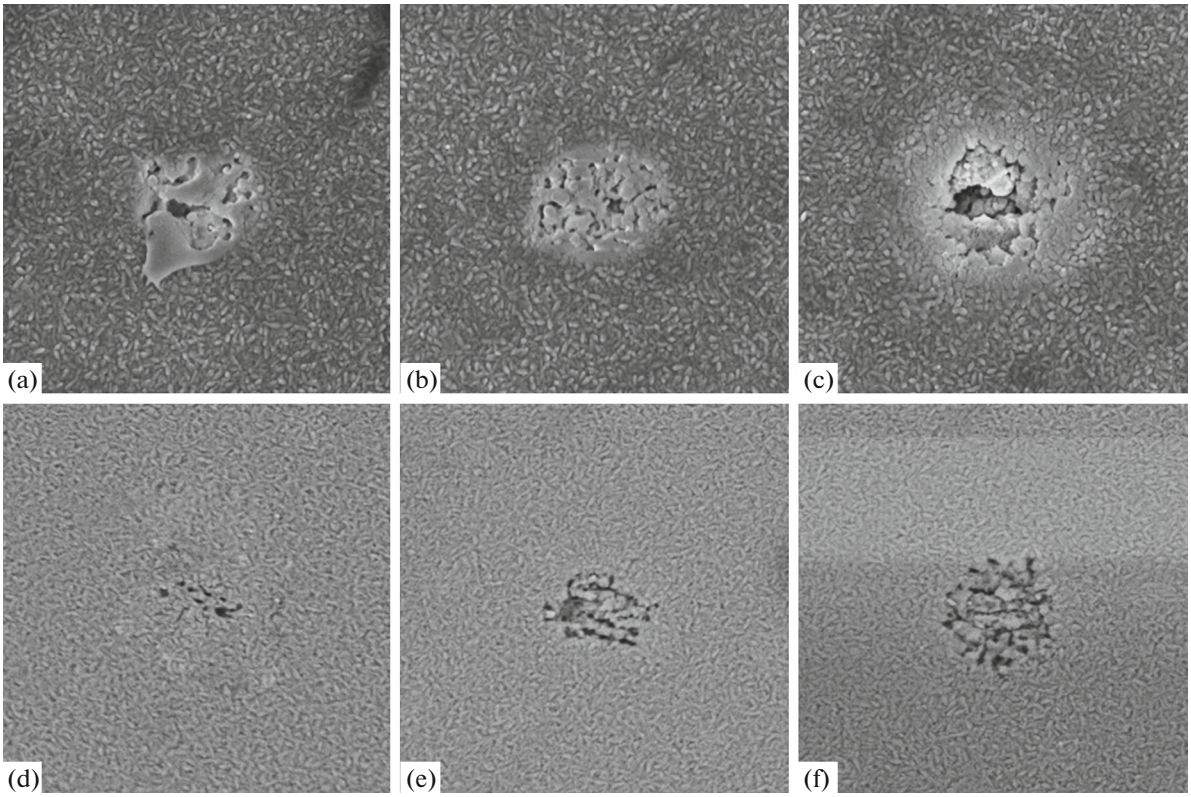

Fig. 1. Scanning electron microscopy images of the surfaces of 3 × 3 μm scan regions of the films with thicknesses of (a–c) 300 and (d–f) 400 nm at annealing times of (a, d) 0.1, (b, e) 1, and (c, f) 10 s.

Earlier [12], we demonstrated the possibility of the formation of local regions of the ferroelectric phase surrounded by a quasi-amorphous precursor. In our previous studies [13, 14], we also used a nonlinear optical technique for controlling the annealing process, which provides a means for detecting second-harmonic signals coming from the ferroelectric phase during and after annealing. This makes it possible to investigate the kinetics of crystallization and to analyze these regions on their nonlinear optical images. Dependences of the optimum parameters of laser annealing on the thickness of the films have not been investigated previously. It is this aspect of the problem that is the subject of the present study.

2. SAMPLE PREPARATION AND EXPERIMENTAL TECHNIQUE

The laser radiation source used in this work was a femtosecond laser (Ti : sapphire, "Avesta Project," Russia) operating at a wavelength of 800 nm with a pulse duration of 100 fs and a pulse repetition rate of 100 MHz. The radiation on the sample was focused using a WITec Alpha 300 confocal microscope with an LD EC Epiplan-Neofluar 100x/0.75 objective. As was shown in our recent study [15], the intensity distribution of the reflected signal at a doubled frequency $I_{2\omega}$ is an indication of the distribution of the ferroelectric perovskite phase. Therefore, the second-harmonic signal was used as a criterion for the presence of the perovskite phase in the sample. The measurements were performed in the "reflection" geometry; i.e., the reflected linear and nonlinear signals were collected using the same objective and directed to the detector. The second-harmonic signal at a wavelength of 400 nm was isolated with a BG-39 color filter. The experiments were carried out using PZT films of the composition $Pb(Zr_{0.54}Ti_{0.46})O_3$ + 10% PbO with thicknesses of 300, 400, 500, and 600 nm [16]. The quasi-amorphous PZT films were deposited by radio-frequency magnetron sputtering on the platinized silicon substrate Pt(80 nm)/SiO_2(300 nm)/Si(300 μm). The average power used in this work was varied in the range from 10 to 20 mW, which under the experimental conditions corresponded to the power density in the range from 0.7 to 1.5 MW/cm^2 and the pulse energy in the range from 0.1 to 0.2 nJ. The ranges of variations in the power density and the exposure time were used to determine the threshold conditions for crystallization. The minimum temperature of crystallization of the PZT compound, according to the experimental data reported in [17], is approximately equal to 700 K. Most frequently, the PZT compound crystallizes at temperatures in the range from 800 to 1000 K. In our study

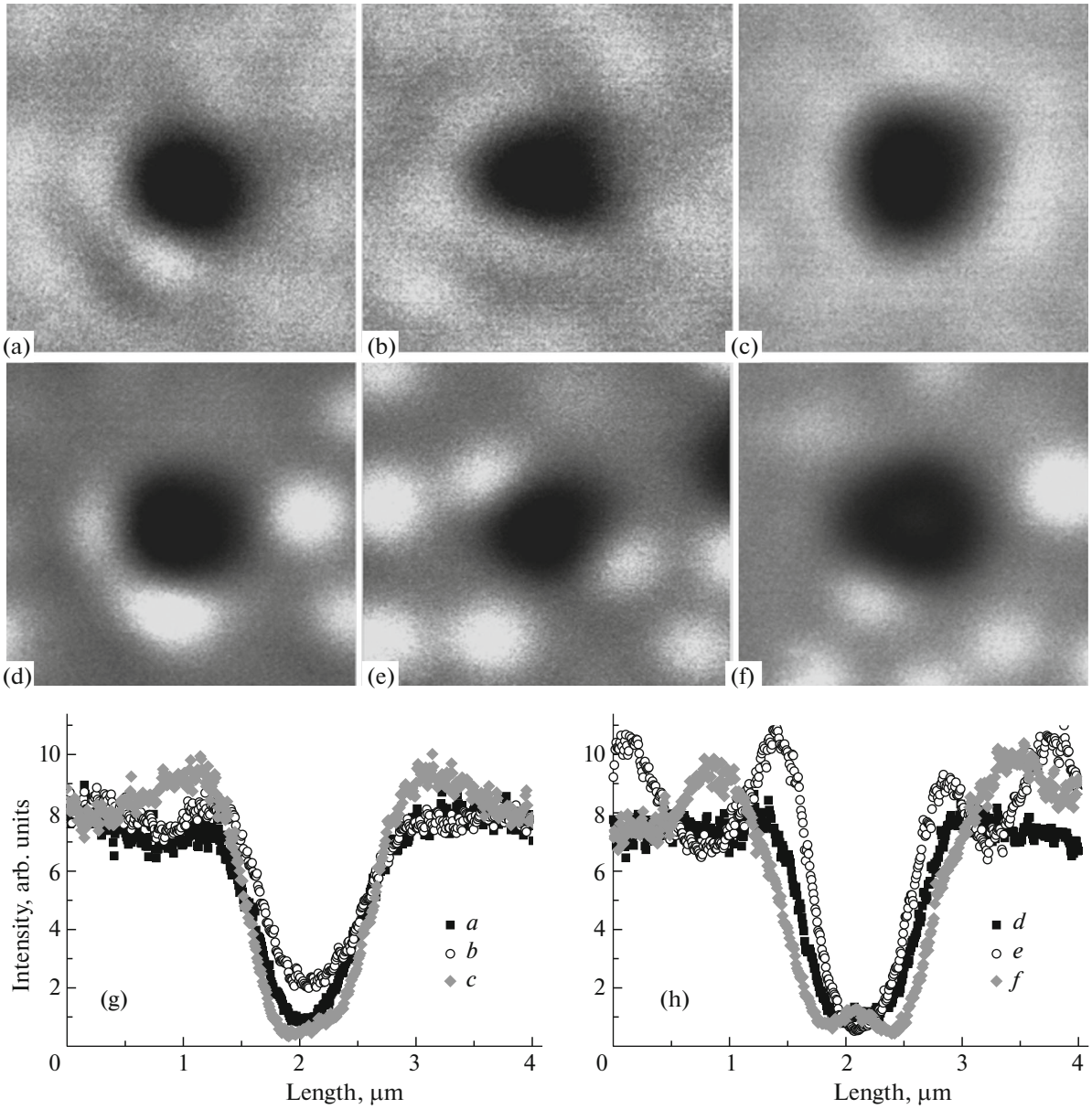

Fig. 2. (a–f) Linear optical images and (g, h) their cross sections for 3 × 3 μm scan regions of the films with thicknesses of (a–c) 300 and (d–f) 400 nm at annealing times of (a, d) 0.1, (b, e) 1, and (c, f) 10 s.

of the laser annealing, we used the minimum possible crystallization temperature in order to avoid undesirable effects. In these experiments, we obtained about 250 local microstructures.

The surface relief of the annealed regions was investigated using the techniques of scanning electron microscopy and atomic force microscopy. The atomic force microscopy images and the images obtained using piezoelectric atomic force microscopy can be found in [18]. In order to investigate the results of annealing throughout the entire thickness of the film, the cross-sectional cleavages in the crystallization regions of the films were examined using transmission electron microscopy [19].

3. EXPERIMENTAL RESULTS AND DISCUSSION

The morphology and sizes of the structures can be evaluated from their scanning electron microscopy images (Fig. 1). The minimum size of the crystallized region of the films was found to be approximately equal to 700 nm (Fig. 1d). These images clearly demonstrate specific features of the surfaces of the films: the central part has a loose structure containing

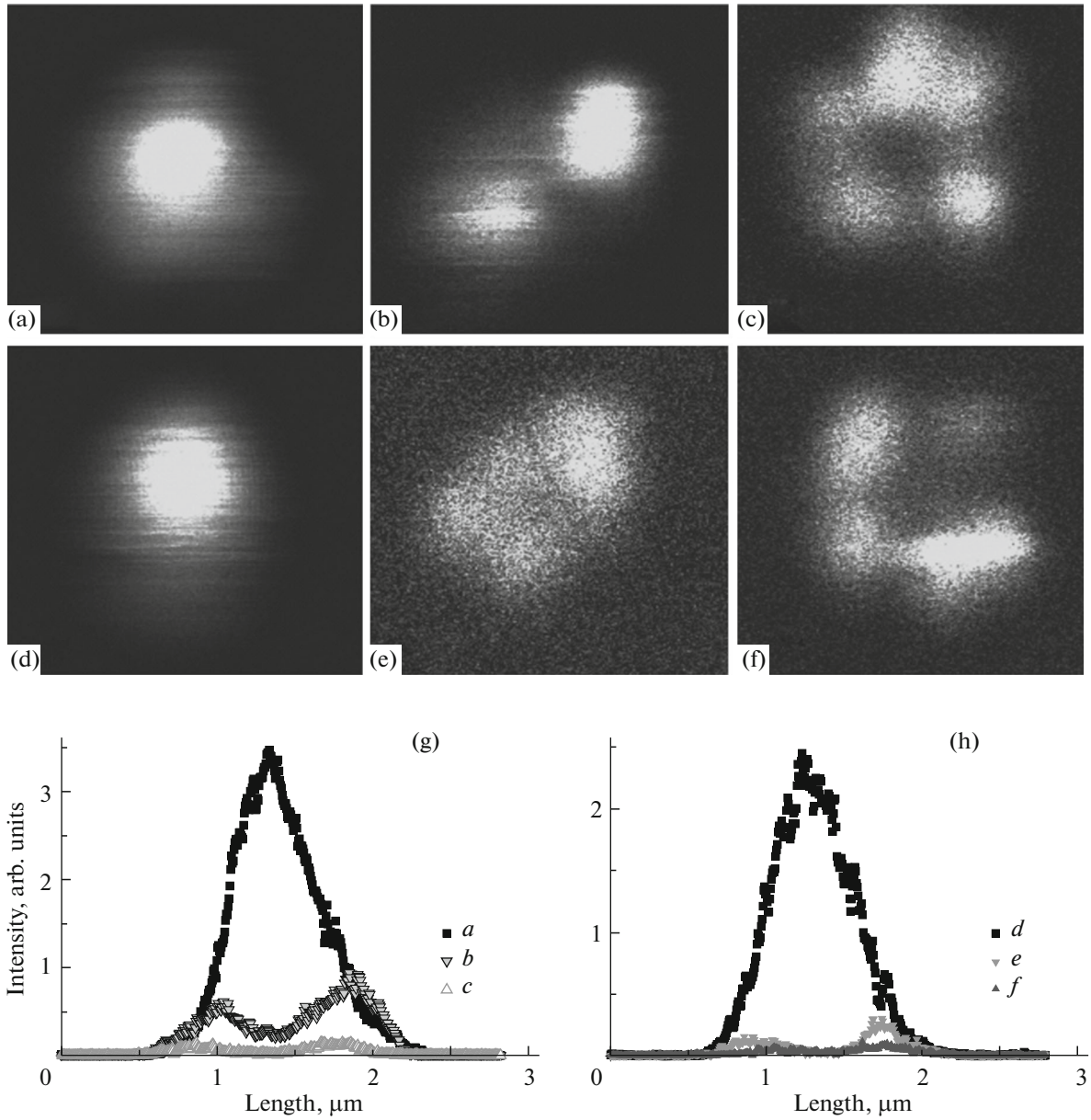

Fig. 3. (a–f) Nonlinear optical images and (g, h) their cross section for 3 × 3 μm scan regions of the films with thicknesses of (a–c) 300 and (d–f) 400 nm at annealing times of (a, d) 0.1, (b, e) 1, and (c, f) 10 s.

smooth sintered regions. The film around the crystallized region consists of small grains.

The confocal images of the crystallized structures for film thicknesses of 300 and 400 nm at annealing times of 0.1, 1, and 10 s are shown in Fig. 2. It can be seen from this figure that the linear optical images contain dark regions corresponding to the crystallization. The contrast with the light background is achieved due to the difference in the refractive indices of the amorphous and crystallized regions. The cross sections of these images (Figs. 2g, 2h) have approximately equal minima in the center of the structures for different durations of annealing and for different film thicknesses. For this reason, it is impossible to reveal the influence of the annealing parameters from the linear optical images.

The crystallization is accompanied by the transition from the centrosymmetric phase (a mixture of the pyrochlore and amorphous phases) to the noncentrosymmetric perovskite phase. Consequently, the crystallized region exhibits the effect of optical second-harmonic generation. Owing to this effect, in the nonlinear optical images (Fig. 3), the central region corresponding to the crystallization looks like a bright spot or several bright spots against the dark background (the absence of the second harmonic in amor-

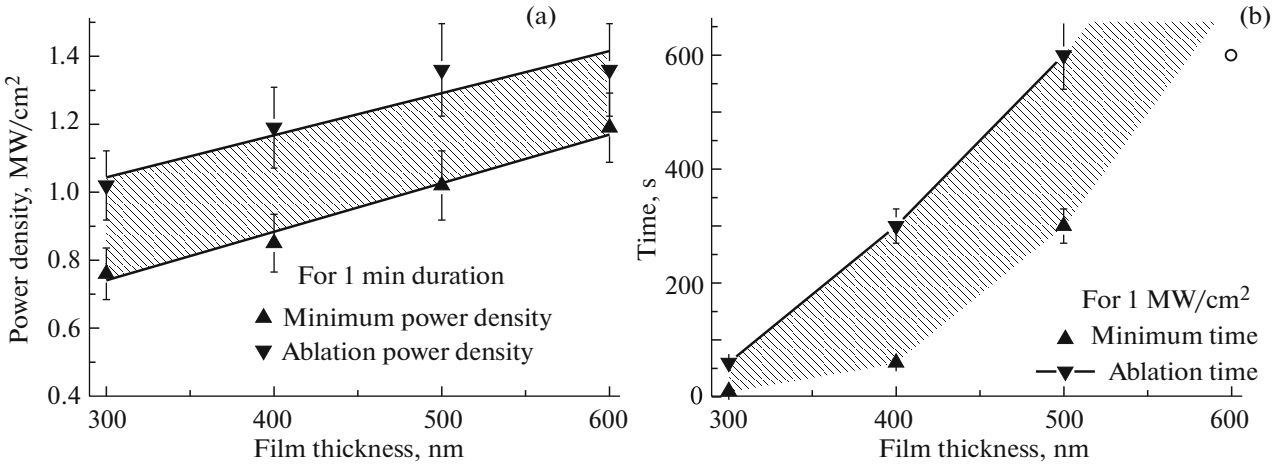

Fig. 4. (a) Range of variations in the optimum power density for crystallization at a given exposure time (1 min) and (b) range of variations in the exposure time at a given power density (1 MW/cm^2) as a function of the thickness of the PZT film.

phous/pyrochlore regions). Considering the presence of such spots in the images, as well as their sizes and shapes, we can judge specific features of the crystallization. The cross sections of these images (Figs. 3g, 3h) serve as a criterion for the quality of the annealing. For the optimum annealing parameters, the cross sections have a Gaussian shape corresponding to the intensity distribution in the laser beam. It can be seen from Fig. 3 that an increase in the annealing time does not lead to an increase in the size of the structures, but the intensity at the center decreases. This is associated with the appearance of undesired effects, such as the ablation, which arises in the center of the structure when the power density and the annealing time exceed the optimum values. The intensity of the second-harmonic signal from the crystallized regions at the shortest duration (0.1 s) of the annealing is almost one order of magnitude higher than the intensity of the others. The average sizes of the structures, according to the estimates made from both the linear and nonlinear optical images, are approximately equal to 1 μm.

The nonlinear optical images allowed us to estimate the lower limit of the power density at which the crystallization begins to occur, as well as the upper limit at which there is an ablation from the central region. Similarly, we determined the limits of durations of the process.

The dependence of the optimum power density for crystallization at a given exposure time (1 min) on the thickness of the PZT film is shown in Fig. 4a. In our case, the parameters above the minimum values sufficient for crystallization and below the values at which the ablation begins to occur are considered to be optimum. With an increase in the film thickness, the minimum power density sufficient for crystallization increases. As the film thickness increases by 100 nm, the required power density increases by approximately 0.1 MW/cm^2. It can be seen from Figs. 4a and 4b that there are three different clearly distinguishable regions. At the bottom of these figures, there is a region in which the power density or the exposure time is not sufficient for crystallization, and a second-harmonic signal is still absent. In the upper region, the experimental conditions lead to an ablation. The middle shaded narrow region is optimum for crystallization. Under these conditions, it is possible to obtain a local ferroelectric region without a defect center.

The dependence of the optimum exposure time for crystallization at a given power density (1 MW/cm^2) on the film thickness is shown in Fig. 4b. With an increase in the thickness of the PZT film, the minimum exposure time sufficient for crystallization also increases. The dependence of the exposure time on the film thickness has a nonlinear character. In particular, the minimum necessary exposure times are equal to 1 min for a film thickness of 400 nm and 5 min for a film thickness of 500 nm, whereas for a film thickness of 600 nm, ten minutes did not suffice for crystallization (this point is marked with an open circle). It can be assumed that, for a particular power density, there is a critical thickness of the film, which already cannot be crystallized throughout the entire thickness, regardless of the exposure time.

In addition to the presented results, we note that the transmission electron microscopy image of the cleavage of the crystallized structure was obtained in [19]. It was shown that the crystallization region is a hemispherical region centered on the surface of the film. It was also demonstrated that the structure contains perovskite and pyrochlore inclusions.

The temperature distribution was evaluated with the COMSOL Multiphysics software package and presented in [12]. The maximum temperature of PZT in the annealing region is approximately 800 K.

4. CONCLUSIONS

In this paper, we have presented the dependences of the optimum parameters of laser annealing for crystallization of local ferroelectric regions without a defect center on the film thickness. With an increase in the film thickness, the annealing time and/or the power density should be increased. Moreover, it should be taken into account that, for the crystallization of thick films, an increase in the annealing time does not always lead to a success, so that it will be necessary to increase the power density and, consequently, the temperature of the process. Presumably, there is a maximum ultimate film thickness throughout which the film can be entirely crystallized using a particular power density. Since the maximum second-harmonic signal was observed in the structures fabricated using a laser annealing for short times (0.1 s), these times can be considered to be optimum for the corresponding power densities.

ACKNOWLEDGMENTS

This study was supported by the Ministry of Education and Science of the Russian Federation within the framework of the State Task to Universities of Russia (project no. 11.144.2014).

REFERENCES

1. K. G. Brooks, I.M. Reaney, R. Klissurska, Y. Huang, L. Bursill, and N. Setter, J. Mater. Res. **9** (10), 2540 (1994).
2. K. H. Park, C. Y. Kim, Y. W. Jeong, H. J. Kwon, K. Y. Kim, J. S. Lee, and S. T. Kim, J. Mater. Res. **10** (7), 1790 (1995).
3. S. Kim, Y. Bastani, H. Lu, W. P. King, S. Marder, K. H. Sandhage, A. Gruverman, E. Riedo, and N. Bassiri-Gharb, Adv. Mater. (Weinheim, Ger.) **23** (23), 3786 (2011).
4. J. Kim, Scanning **32**, 320 (2010).
5. Y. Matsui, M. Okuyama, N. Fujita, and Y. Hamakawa, J. Appl. Phys. **52** (8), 5107 (1981).
6. C.-F. Chou, H.-C. Pan, and C.-C. Chou, Jpn. J. Appl. Phys., Part 1 **41** (11B), 6679 (2002).
7. S. A. Akhmanov, V. I. Emel'yanov, N. I. Voroteev, and V. N. Seminogov, Sov. Phys.—Usp. **28** (12), 1084 (1985).
8. M. H. M. Zai, A. Akiba, H. Goto, M. Matsumoto, and E. M. Yeatman, Thin Solid Films **394**, 96 (2001).
9. A. Queraltó, A. P. del Pino, M. de la Mata, J. Arbiol, M. Tristany, A. Gómez, X. Obradors, and T. Puig, Appl. Phys. Lett. **106** (26), 262903 (2015).
10. J. P. B. Silva, A. Khodorov, A. Almeida, J. A. Moreira, M. Pereira, and M. J. M. Gomes, Appl. Phys. A: Mater. Sci. Process. **116** (3), 1271 (2014).
11. H. Palneedi, D. Maurya, G.-Y. Kim, S. Priya, S.-J. L. Kang, K.-H. Kim, S.-Y. Choi, and J. Ryu, Appl. Phys. Lett. **107** (1), 012904 (2015).
12. A. S. Elshin, N. Yu. Firsova, E. D. Mishina, D. A. Abdullaev, and D. A. Kiselev, Vestn. Mosk. Inst. Radiotekh., Elektron. Avtom. **4**, 230 (2014).
13. A. S. Elshin, N. Yu. Firsova, M. A. Marchenkova, V. I. Emel'yanov, I. P. Pronin, S. V. Senkevich, E. D. Mishina, and A. S. Sigov, Tech. Phys. Lett. **41** (5), 418 (2015).
14. N. Yu. Firsova, A. S. Elshin, M. A. Marchenkova, A. K. Bolotov, M. S. Ivanov, I. P. Pronin, S. V. Senkevich, D. A. Kiselev, and E. D. Mishina, Nano- Mikrosist. Tekh., No. 7, 43 (2014).
15. N. E. Sherstyuk, E. D. Mishina, S. D. Lavrov, A. M. Buryakov, M. A. Marchenkova, A. S. Elshin, and A. S. Sigov, Ferroelectrics **477**, 29 (2015).
16. I. P. Pronin, E. Yu. Kaptelov, S. V. Senkevich, V. A. Klimov, N. V. Zaitseva, T. A. Shaplygina, and S. A. Kukushkin, Phys. Solid State **52** (1), 132 (2010).
17. C. K. Kwok and S. B. Desu, J. Mater. Res. **8** (2), 339 (1993).
18. A. S. Elshin, N. Yu. Firsova, E. D. Mishina, O. M. Zhigalina, D. A. Abdullaev, and D. A. Kiselev, Nanomater. Nanostrukt.—XXI Vek, No. **3**, 30 (2014).
19. A. S. Elshin, I. P. Pronin, O. M. Zhigalina, M. Yu. Presniakov, D. N. Khmelenin, E. D. Mishina, and V. I. Emel'yanov, Solid State Commun. (2016) (in press).

Translated by O. Borovik-Romanova